Z. Phys. Chem. **224** (2010) 761–779 / **DOI** 10.1524/zpch.2010.5484

Evidence for Vibrational Excitation of the Adlayer in Exoergic Processes at Metal Surfaces: H-atom Abstraction and Recombination and Adsorption-stimulated Desorption of CO

By E. Molinari and M. Tomellini*

Dipartimento di Scienze e Tecnologie Chimiche, Università di Roma Tor Vergata, Via della Ricerca Scientifica, 00133 Roma, Italy

(Received April 29, 2010; accepted October 22, 2010)

Kinetics of Surface Reactions / Non-equilibrium Phenomena / Atom Recombination / Catalysis

The theoretical model presented in the previous paper predicts the possibility of vibrational excitation of the adlayer in exoergic process at metal surfaces to an extent determined by the interplay of reaction rates and energy dissipation into the metal. In the present paper this model will be employed for studying the following systems: a)The abstraction of D_s adspecies by H_{gas} and the accompanying H-atom recombination and b) the adsorption-stimulated desorption of CO_s in the presence of adsorbing CO_{gas}. Proper reduction of literature data provides the evidence for the existence of vibrational excitation of the H-Me and of the CO-Me adlayers, witnessed by desorption rates that are orders of magnitude larger than those expected for systems in Boltzmann equilibrium. Application of the model to D_s+H_{gas} relates the vibrational excitation of the adlayer and the corresponding non-Boltzmann desorption rates to the parameter Z/K and to the flux of adsorbing species. Rate coefficients K for vibrational relaxation of the H-Me bond are in the range 10^{13}-10^{12} s^{-1} and decrease with increasing surface coverage σ. The analysis of CO_s desorption in the presence of adsorbing CO_{gas} confirms the dependence of desorption rates on Z/K, the coverage dependence of the rate coefficients K for energy relaxation of the CO-Me bond and brings out the predicted influence of gas pressure on the *over*-population of the vibrational levels of adsorbed CO. The decrease of K observed in both systems is discussed in terms of energy relaxation processes involving electron-hole pair excitation at the metal surface and it should be linked to the decrease of the surface electron density caused by the adsorbates.

* Corresponding author. E-mail: tomellini@uniroma2.it

1. Introduction

Within the framework of the theoretical model developed in the previous paper [1] we examine two distinct classes of stimulated desorption processes at a metal surface:

a) *Reaction-stimulated desorption* (*rsd*): The model will be employed for the analysis of experimental data on D_s abstraction by H_{gas} atoms with the accompanying exoergic H-atom recombination.

b) *Adsorption- stimulated desorption (asd):* The controversial phenomenon of enhanced CO_s desorption from metal surfaces in the presence of adsorbing CO_{gas} will be presented and analysed according to the theoretical model.

Let us begin with recalling the basic results of ref.[1] that are relevant to desorption processes occurring in parallel to a progressive increase of surface coverage

1.1 Reaction-stimulated desorption, recombination (rsd)

We refer to a *harmonic* vibrational ladder of the *H*-adatom, and consider atom recombination to arise from a performing level $j = p$ of energy $E_p = 2E_a = E^{\#}$ (E_p is measured from the ground level $j = 0$, $-2E_a$ is the adsorption energy of $H_{2\,gas}$, $E^{\#}$ the activation energy of the desorption process), according to $H_p + H_0 \rightarrow H_{2gas}$, and from level $j = p/2$ at $E_{p/2} = E_a$ according to $H_{p/2} + H_{p/2} \rightarrow H_{2gas}$.

For the desorption (recombination) rate$/\mathrm{MLs}^{-1}$ one than writes $\Phi = 2Z\sigma_0\sigma_p + 2(\frac{Z}{2})\sigma^2_{p/2}$. For an exponential vibrational distribution function, $\sigma^2_{p/2} = \sigma_p$ and one receives $\Phi = 3Z\sigma_0\sigma_p$ where σ_0, σ_p, $\sigma_{p/2}$ are the fractional surface coverages by H-adatoms in levels $j = 0$, p, $p/2$ respectively.

The model provides the population of level p according to

$$\sigma_p = \sigma_0\gamma_B^p + \left(\frac{\Phi}{3} + \dot{\sigma}\right)\frac{1}{K} \tag{1}$$

where $\gamma_B^p = e^{-\beta p E_{01}}$ the Boltzmann factor, $\dot{\sigma} = d\sigma/dt$ and K the rate coefficient for energy transfer in a VL process. This is a basic equation of the model, showing that the population of the performing level p is larger than the Boltzmann one. This is accounted for by the last term in eqn.1, which depends on the total flux of the adsorbing atoms and on the efficiency of VL transfer. The model then provides the expression for the recombination rate Φ (eqn.15 of [1]),which, for a highly efficient VV scattering, becomes

$$\Phi = \frac{\Phi_B + 3\dfrac{Z\sigma_0\dot{\sigma}}{K}}{1 - \dfrac{Z\sigma_0}{K}} \tag{2}$$

where $\Phi_B = 3Z\sigma_0^2\gamma_B^p$ is the desorption rate for a system in Boltzmann equilibrium and $\sigma_0 \cong \sigma$.

In the case of vibrational relaxation via electron-hole (e-h) pair excitation the rate coefficient K has been reported in [1]. It was shown that, for a single e-h pair

excitation, $K_{v',v} \cong \rho^2 \Gamma_{\Delta E} \Delta E$ whith v,v' adatom vibrational quantum numbers, $\Delta E = E_{v'} - E_v$ the energy transferred to the solid, ρ the electron density of states and $\Gamma_{\Delta E}$, the transition probability, is a function of ΔE. With n_e/cm^{-3} electron density and $\varepsilon_F/\mathrm{eV}$ the Fermi energy, one writes

$\rho = n_e/\varepsilon_F = 3 \times 10^{14} n_e{}^{1/3}/\mathrm{eV}^{-1}\,\mathrm{cm}^{-3}$, and receives

$$K_{v',v} \propto n_e^{2/3} \Gamma_{\Delta E} \Delta E. \tag{3}$$

The rate constant for the reverse process, i.e. the vibrational excitation of the H-adatom by the (e-h) pair, $K_{v,v'}$, is linked to $K_{v',v}$ by the detailed balance. For an electron bath in thermal equilibrium one writes $K_{v,v'} = K_{v',v}\, e^{-\beta \Delta E}$. It was shown in [1,2], however, that the distribution function of the electrons is affected by the exoergic process and the detailed balance becomes $K_{v,v'} = K_{v',v}\,(e^{-\beta \Delta E} + \chi\Phi)$ with χ given by eqn.30 of [1]. This additional term depends on the recombination rate Φ and might exceed the Boltzmann term by orders of magnitude [2].

The effect of the hyperthermal electron distribution function on the reaction rate has been investigated in [1,2]. The upper bound of the recombination rate is estimated as

$$\Phi = \frac{\left[\Phi_B + 3Z\sigma_0 \dot{\sigma}\left(\chi\sigma(1+\eta) + K^{-1}\right)\right]}{[1 - Z\sigma_0 K^{-1}(1 + 3\sigma\chi K)]} \tag{4}$$

where $\eta = 2E_a/D_{H_2}$, D_{H_2} dissociation energy of H_{2gas} and the upper bound of the adatom population reads

$$\sigma_p = \sigma_0 (\gamma_B + \chi\Phi)^p + \left(\frac{\Phi}{3} + \dot{\sigma}\right)\frac{1}{K}. \tag{5}$$

The condition of efficient VV transfer in the adlayer leads to vibrational distribution functions that can be described by the equation

$$\frac{\sigma_j}{\sigma_0} = \exp\left(-\beta j E_{01}\left(\frac{T}{T_1} - \delta(j-1)\right)\right), \tag{6}$$

with δ the anharmonicity of the potential well, $\beta = \frac{1}{k_\beta T}$ and $T_1 > T$ a measure of the *over*population of the levels compared with the Boltzmann distribution. Eqn.6 exhibits a minimum at $j = \frac{T_s}{2\delta T_1} + \frac{1}{2}$. For a harmonic ladder ($\delta = 0$) eqn.6 becomes

$$\frac{\sigma_j}{\sigma_0} = \exp\left(-\beta j E_{01}\left(\frac{T}{T_1}\right)\right), \tag{7}$$

where $(\frac{T}{T_1})$ is related to the physical quantities of the adsorption-recombination process [1].

1.2 Adsorption-stimulated desorption (asd)

The influence of the adsorption rate $\frac{d\sigma}{dt} = \dot{\sigma}$ on the vibrational distribution function of the adsorbate is expressed by $\sigma_p = \sigma_0(\gamma_B + \chi'\dot{\sigma})^p + \frac{\dot{\sigma}}{K}$ where $E_p = E_a$ is the adsorption energy. By neglecting the χ' containing terms, the desorption rate, $\Phi = Z'\sigma_p$ reads

$$\Phi - \Phi_B = \Phi_{asd} = \frac{Z'\dot{\sigma}}{K} \tag{8}$$

with $\Phi_B = Z\dot{\sigma}\gamma_B^p$ and Z' is the rate constant for desorption.

2. Applications of the model

2.1. Reaction-stimulated desorption (rsd): abstraction of chemisorbed D_s species by gas H-atoms

The kinetics of D-adatom abstraction by gas H-atoms was investigated, among others, at Pt(111) [3, 4], Pt(110) [5], Ni(100)[6] and Cu(111) [7] surfaces. Rates of D-adatom abstraction as HD and D_2 molecules from surfaces, partially or totally covered by pre-adsorbed deuterium, were studied as a function of time at a constant flow of H gas atoms. Recombination of H and of D adatoms occurs according to a Langmuir–Hinshelwood mechanism while the total coverage by H_s+D_s increases from the initial value, $\sigma(0)_D$, corresponding to the amount of preadsorbed D_s, to surface saturation by H_s at steady state σ_{ss}.

By proper reduction of these data [8] one derives the *total* recombination rate, Φ, of the adatoms as HD, D_2 and H_2 molecules, the H-atom adsorption rate $\dot{\sigma} = \dot{\sigma}(0)(1-\sigma)$ and the total flux of adsorbing H-atoms $J = \dot{\sigma} + \Phi$, as a function of surface coverage σ. In fig.1, Φ, $\dot{\sigma}$, J in MLs^{-1} units, have been plotted vs. σ for the four systems examined. At the temperatures of the experiments (100 ± 20 K) and with activation energies $E^{\#} = 2E_a$ in the range 70–110kJmol^{-1}(ref.[8] and Table1) the condition $\Phi_B \ll \Phi$ is satisfied for all systems. From eqn.4, which relates the parameters of the model Z, K and χ, to the experimental quantities Φ, $\dot{\sigma}$ and σ one receives, in case of a negligible contribution of χ containing terms,

$$K = \frac{Z\sigma(3\dot{\sigma} + \Phi)}{\Phi}. \tag{9}$$

From the plots of fig.1, employing the reasonable value Z = 10^{12} s^{-1} together with eqn.9, one gets the log K vs. σ plots of fig.2 which become linear above given σs. Initial deviations from linearity in the log K vs. σ plots of fig.2 (dashed lines) should be attributed, according to [8], to non-steady state conditions prevailing while the system relaxes from initial overpopulation spikes. Slopes b of the linear part of these plots have been included in table 1 and will be examined

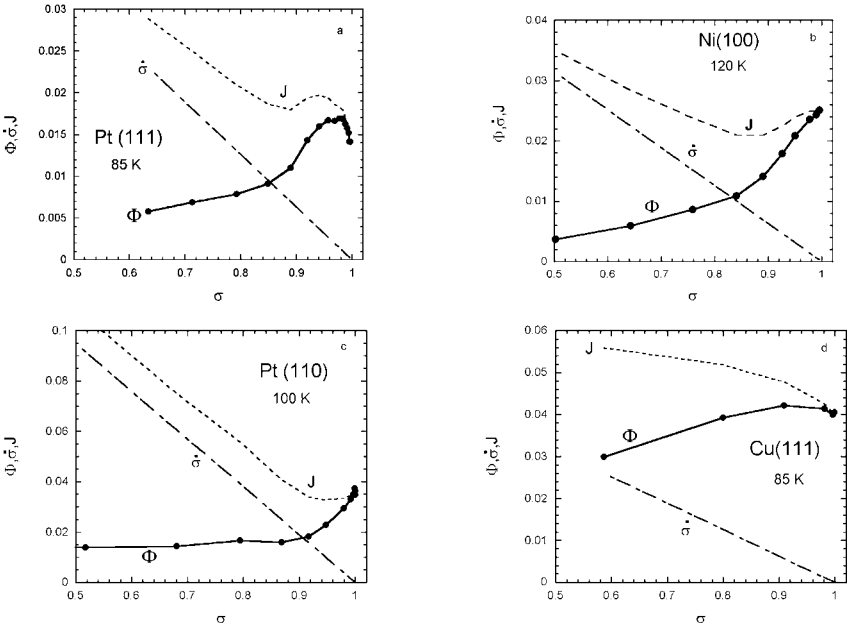

Fig. 1. *Abstraction of chemisorbed D_s species by gas H-atoms.* Plots of the total desorption rate, Φ, of the H adsorption rate, $\dot{\sigma}$, and of the total flux of adsorbing H atoms, J, (in MLs^{-1} units) vs. total surface coverage σ for the systems and the temperatures marked in the panels a-d: Pt(111), $\dot{\sigma}(0) = 0.063$, $\sigma_D(0) = 0.61$; Ni(100), $\dot{\sigma}(0) = 0.063$, $\sigma_D(0) = 0.47$; Pt(110), $\dot{\sigma}(0) = 0.19$, $\sigma_D(0) = 0.55$; Cu(111), $\dot{\sigma}(0) = 0.063$, $\sigma_D(0) = 0.56$.

Table 1. Kinetic parameters for H+D_s ($Z = 10^{12}s^{-1}$).

Surface	T/K	$E^{\#}$/kJmol^{-1}	T/T_1	b
Pt(111)	85	70	0.34	3.4
Pt(110)	100	110	0.27	(3.9)
Ni(100)	120	104	0.32	3.2
Cu(111)	85	92	0.27	1.2

in the discussion section. The b value for Pt(110) refers to a linear log K vs. σ^2 plot.

Values of χ can be calculated from eqn.30 of [1] and, when inserted in eqn.4, do actually make a negligible contribution to the desorption rates Φ, except for Pt(111). These values of χ do represent, however, an upper bound, as discussed in [1], so that the contribution of χ containing terms, can always be neglected. These terms represent the contribution to the *over*population of the performing vibrational levels of the adatoms of the energy *back* pumping into the adlayer from *hyper* thermal electrons generated by the exoergic process. This contribu-

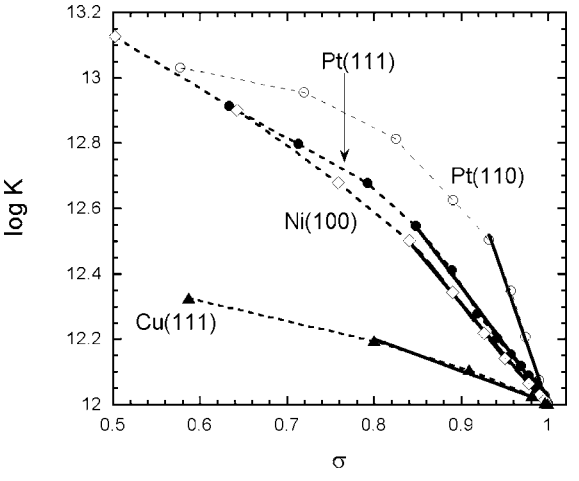

Fig. 2. *Abstraction of chemisorbed D_s species by gas H-atoms*. plots of the logarithm of the rate constant for vibrational relaxation, K, vs. total surface coverage σ for the various systems.

tion can therefore be neglected, at least for the range of Φ values here considered (eqn.5)

From $\Phi(\sigma)$ and $J(\sigma)$ of fig.1 and $K(\sigma)$ of fig. 2 one calculates Φ/J vs. Z/K as plotted in fig.3 for the different systems. From eqn.4 one also obtains $\frac{\Phi}{J} = (\frac{Z}{K(\sigma)})(\frac{(3\dot{\sigma}+\Phi)}{(\dot{\sigma}+\Phi)})\sigma$. At s.s. $\dot{\sigma} = 0, \sigma = 1, \Phi_{ss} = J_{ss}$ and $(\frac{Z}{K})_{ss} = 1$ as shown in fig.3.

The kinetic analysis of ref.[8] provids the time evolution up to s.s. (steady state) of the populations of three selected vibrational levels. From the relative populations of these levels at s.s. it was possible to determine, according to eqn.6, both E_a and the non-equilibrium parameter T/T_1. Values of $E^{\#} = 2E_a$ have been included in Table 1 together with T/T_1 as recalculated for the harmonic oscillator considered in the present analysis (δ = 0, eqn.7) from the values of Table 1 of ref. [8] determined for an anharmonic oscillator (δ = 0.015). From the data of Table 1 one obtains the distribution functions, shown in fig.4 together with the corresponding Boltzmann distributions. This figure should be compared with fig.4 of [1].

2.2. Adsorption-stimulated desorption (asd): desorption rates of CO_s in the presence of CO_{gas}

The experimental data of refs. [10–14] for the systems CO-Me (Me = Pd, Rh, Ni foils and Ni and Ru single crystals), of ref.[15] for H-W and of ref.[16] for (NH_3+H_2)-Fe, provide evidence for the *stimulation* of the desorption processes of CO, H_2 and NH_3 by the adsorbing species. In fact, the various 'isotope jump'

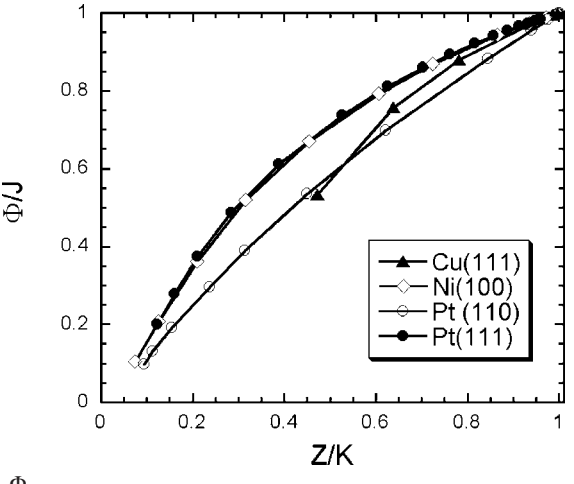

Fig. 3. The ratio $\frac{\Phi}{J}$ has been plotted as a function of Z/K for the various systems.

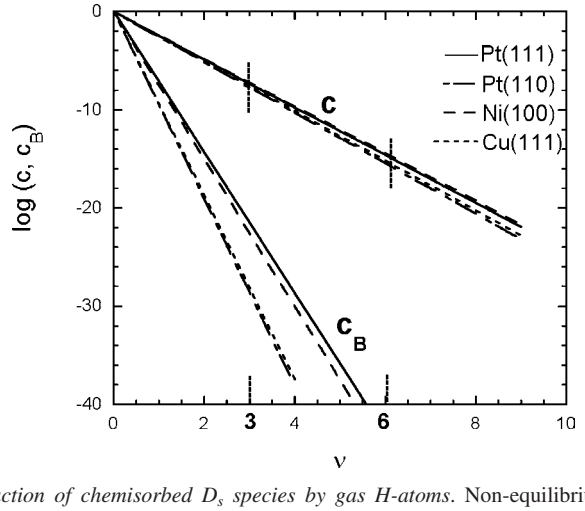

Fig. 4. *Abstraction of chemisorbed D_s species by gas H-atoms*. Non-equilibrium vibrational distribution functions $c(v)$ and corresponding Boltzmann distributions $c_B(v)$ for the various systems (harmonic vibrational ladders with $E_{01} = E^{\#}/6$ and $E^{\#}$ from Table 1).

methods utilised in these experiments did show that desorption rates measured *in the presence of the adsorbing gas* were approximately proportional to the pressure of this gas and could be much higher than those obtained under vacuum conditions at the same temperature. More recent results [17] on the CO-Ir (111) system have shown, however, that rates of desorption measured *under strict*

equilibrium conditions of the adsorption process coincide with those measured in vacuo, i.e. there was apparently no evidence for *asd*. *Asd* is seemingly a rather puzzling phenomenon, as maintained in [18].

In the present analysis we shall focus on the experimental data available for CO desorption from refs.[10–14,17] and show how to apply the non-equilibrium model to these data.

2.2.1. Reduction of experimental data

From the experiments of refs.[10–14] one receives the rates of $^{12}C^{16}O$ adsorption, $\dot{\sigma} = d\sigma/dt$, the net desorption rate of $^{12}C^{18}O$, Φ, (as obtained at a pressure p of the lighter isotope present in the gas phase while measuring the desorption rate of the previously adsorbed heavier isotope), and $J = \dot{\sigma} + \Phi$. In fig.5, $\dot{\sigma}$, Φ, $J = \dot{\sigma} + \Phi$, in units10^{-2} MLs^{-1}, have been plotted as a function of the fractional surface coverage σ. Experimental desorption rates $\Phi(\sigma)$ can always be fitted by straight lines and their slopes depend on the pressure p of the adsorbing $^{12}C^{16}O$ according to a power law $d\Phi/d\sigma = k_{des} \propto p^q$, with q within the range 0.7–0.9. The observed adsorption rates $\dot{\sigma}$ (σ) for Pd, Ni and Rh foils can satisfactorily be fitted, at all temperatures, by the equation,

$$\dot{\sigma} = \dot{\sigma}_0(1-\sigma'^m) \tag{10}$$

with $\sigma' = \sigma \,/\, \sigma_{eq}$, $m = m(T)$ which can be preceded by an initial steeper decay. Adsorption rates for Ru(0001) are better described by the expression

$$\dot{\sigma} = \dot{\sigma}_0\left(1+\frac{n\sigma'}{(1-\sigma')}\right)^{-1} \tag{11}$$

with $n = n(T)$. Values of m (eqn.10) and of n (eqn.11) for the various systems and temperatures have been collected in Table 2.

The fractional surface coverage σ was defined in refs.[10–14] as $\sigma = N(p,T,t) \,/\, N_0$, with N_0 number of adsorbed CO molecules per cm^2 of the metal target at saturation, as derived at the lowest temperature T and at the maximum pressure p of the experiments. This implies that units MLs^{-1} (1ML = N_0) are not immediately comparable among the various systems since N_0, as defined above, doesn't necessarily coincide with the maximum ideal coverage M of the given surface by adsorbed CO species, also in view of the surface roughness of the foils used in the experiments. In order to make the comparison among the various systems reliable, a standard criterion for the evaluation of $M \neq N_0$ has been adopted. By taking, as suggested by literature data, $M = 0.5M_0$, corresponding to an ideal c(2x2) structure of adsorbed CO on a (111) or (100) surface, with M_0/metal-atoms cm^{-2}, one easily derives $\frac{rM}{N_0} = \mu = \frac{\sigma_{\exp}}{\sigma_c} = \frac{\dot{\sigma}_{\exp}}{\dot{\sigma}_c} = \frac{\Phi_{\exp}}{\Phi_c} \geq 1$ with $r \geq 1$ roughness factor of the surface and M_0 averaged between a (111) and a (100) surface. The "correct" values σ_c, $\dot{\sigma}_c$, Φ_c are given by the experimental ones $\sigma_{\exp}$, $\dot{\sigma}_{\exp}$, Φ_{exp} divided by $\mu \geq 1$. In the following we shall employ the "correct" values of these quantities.

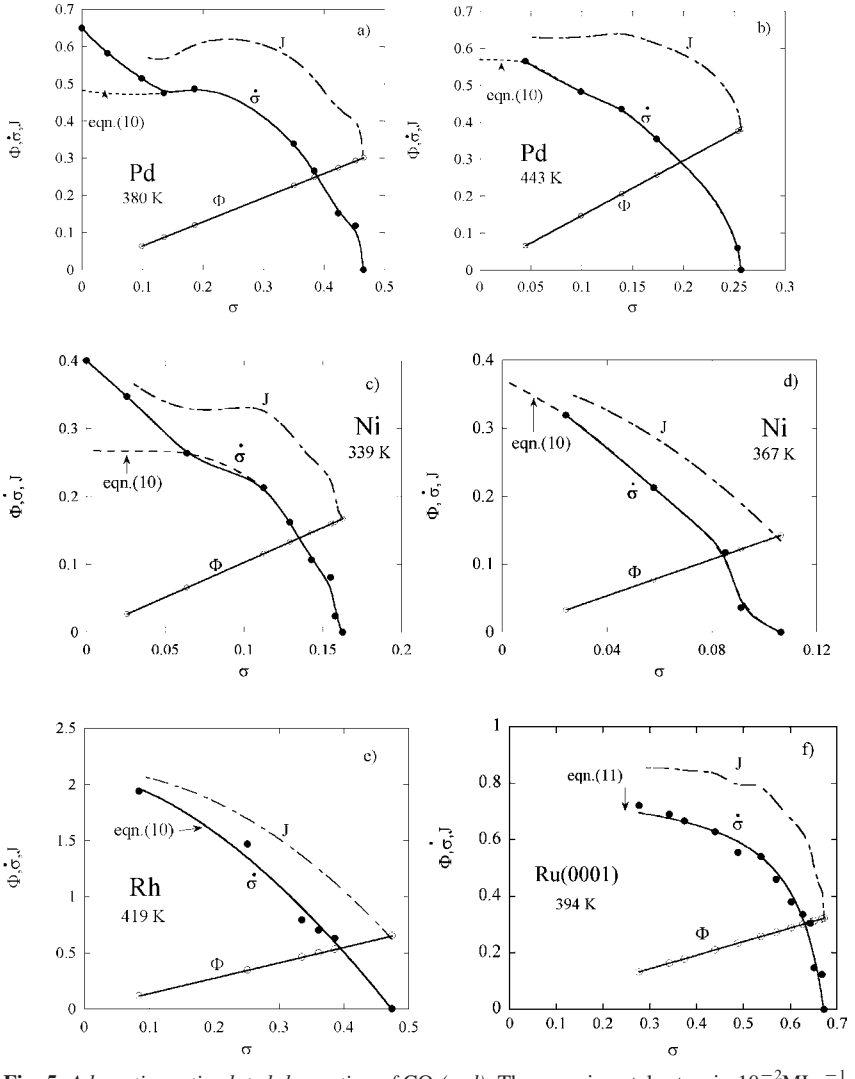

Fig. 5. *Adsorption- stimulated desorption of* CO *(asd).* The experimental rates, in 10^{-2}MLs^{-1} units, for CO adsorption, $\dot{\sigma}$, and desorption, Φ, have been plotted as a function of the fractional surface coverage by CO_s, σ. In the same panel the quantity J = (Φ+$\dot{\sigma}$) is also displayed. Panels (a,b): Pd(foil) at T = 380 K and 443 K, respectively, at $p = 2\times10^{-6}$ Pa. Panels (c,d): Ni (foil) at 323 K and 339 K, respectively, at p = 1.3. Panel (e): Rh (foil) at 419 K at p = 7.3. Panel (f): Ru(0001) at 394 K and p = 2.4. Fitting of $\dot{\sigma}$ vs. σ curves has been done through eqn.10 in panels (a-e) and through eqn.11 in panel (f). Corresponding values of *m(n)* can be found in Table 2.

Table 2. Asd-CO: σ_{eq},m(n),log K(0), b, $p/10^{-6}$Pa, $g/10^{-2}$ mol kJ^{-1},W/eV, Z' = $5 \times 10^{13} s^{-1}$.

T/K	σ_{eq}	m(n)	LogK(0)	b	g
Pd(foil)(p = 2,W_{exp} = 0.9 ± 0.1)					
380	0.45	4.4	14.8	2.7	6.9
443	0.25	2.5	14.7	4.0	4.9
466	0.20	1.2	14.7	6.4	—
Ni(foil)(p = 1.3,W_{exp} = 1.3 ± 0.2)					
323	0.20	2.0	14.9	7.4	4.9
339	0.16	4.3	14.9	8.2	4.8
367	0.11	1.4	14.8	13	—
394	0.06	1.0	14.8	20	—
Rh(foil)(p = 7.3,W_{exo} = 1.0 ± 0.1)					
394	0.6	2.8	15.15	2.2	11.5
419	0.5	1.6	15.12	3.3	9
Ru(0001)(p = 2.4,W_{exp}n.a.)					
394	0.7	n = 0.1	15	1.31	—
418	0.6	n = 0.2	14.4	2.1	—

The $E_a(\sigma)$ function can be determined from experimental rates of desorption measured at equilibrium

$$\Phi\ (\sigma_{eq}, T) = \sigma_{eq} Z' \exp(-\beta E_a(\sigma_{eq})) = k_{des}\sigma_{eq}. \tag{12}$$

The expression of Φ will then be written as

$$\Phi = \sigma(Z' \exp(-\beta E_a(\sigma)) + k_{asd}) = \sigma(k_B + kp^q) = k_{des}\sigma, \tag{13}$$

where the rate coefficient of adsorption stimulated desorption k_{asd} is given by

$$k_{asd}\sigma = (\Phi - \Phi_B) = \Phi_{asd} \quad \text{and}$$
$$\Phi_B = \sigma Z' \exp(-\beta E_a(\sigma)). \tag{14}$$

In the following the value $Z' = 5 \times 10^{13}$ s^{-1}, within the extended literature range (10^{13}-$10^{16} s^{-1}$), will be employed. This value is of the order of magnitude of the vibrational stretching frequencies of Me-CO surface bonds [19]. The desorption energies $E_a(\sigma)/\text{kJmol}^{-1}$ of CO can be calculated as a function of σ by employing eqn.12 with k_{des} and σ_{eq} available from the experiments at various temperatures. One is then in a position to estimate $\Phi_B(\sigma)$ at the temperatures of interest.

Fig.6 shows the adsorption energies E_a, derived from eqn.12, as a function of σ. The extrapolated points at σ = 0 for Pd and Ni foils are mean values of

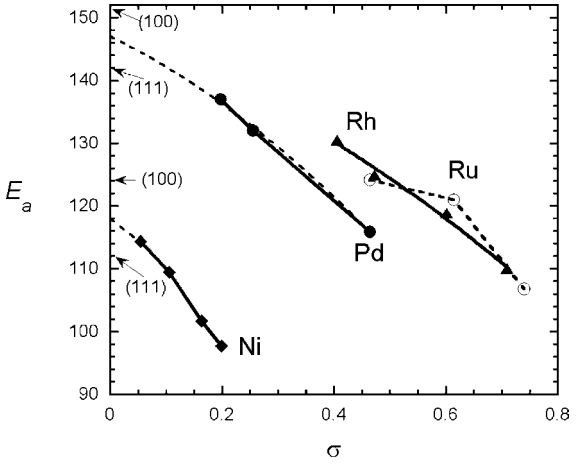

Fig. 6. CO *asd.* The desorption energy E_a /kJmol^{-1} is plotted as a function of the fractional surface coverage σ, for Ni (foil), Pd (foil), Rh (foil), Ru (0001) (see text).

E_a determined for Pd(111) and Pd (100) in ref.[20] and for Ni(111) and Ni(100) in ref.[21].

Plots of Φ, Φ_B, Φ_{asd} as a function of σ, are shown in fig.7(a) for Pd (T/K = 380 and 466, p/10^{-6}Pa = 2), which are representative of a general behaviour. Desorption rates $\Phi\sigma$ have been measured at five pressures between 1.3×10^{-6} Pa and 13×10^{-6} Pa on the Pd foil and fig.7(b) shows $\Phi_{asd}(\sigma) = \Phi(\sigma) - \Phi_B(\sigma)$ at 380 K at the various pressures, together with the *pressure independent* $\Phi_B(\sigma)$. With $c^* = \sigma^*/\sigma_0 \cong \sigma^*/\sigma$ the relative population of CO adspecies in the upper vibrational level ν^* at energy $E_{\nu^*}(\sigma)$, one writes for the monomolecular rates of desorption, $\Phi = Z'\sigma c^*$, $\Phi_B = Z'\sigma c^*_B$, $\Phi_{asd} = Z'\sigma c^*_{asd}$, with $c^* = c^*_B + c^*_{asd}$ and $c^*_B = \exp(-\beta E_a(\sigma))$. Fig.8 illustrates the dependence of these quantities on σ for Pd at two temperatures. One also defines $f = c^*/c^*_B$, a measure of the *over*-population of level ν^* with respect to the Boltzmann distribution. Fig.9a shows log f vs. σ for the Ni foil at different temperatures and $p = 1.3\times10^{-6}$ Pa and fig.9b the function log f vs. σ, at various pressures and T = 339K.

2.2.2 Application of the model

Eqn.8 is the basic result of the non-equilibrium model for *asd*. Under present conditions the term χ' can be neglected and one receives

$$K(\sigma) = Z' \frac{\dot{\sigma}}{\Phi_{asd}}. \tag{15}$$

With $Z' = 5\times10^{13}$s^{-1}, selected as specified above, one calculates the dissipation rate constant $K(\sigma)$ from properly smoothed experimental Φ_{asd} and $\dot{\sigma}$ at the available temperatures. Fig.10a shows the results for Pd and fig.10b for Ni. These

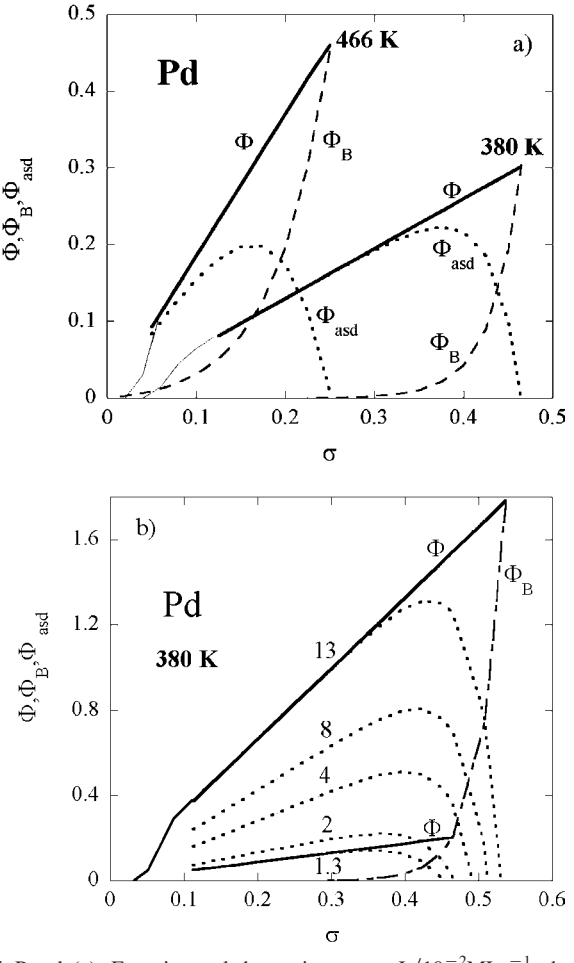

Fig. 7. CO *asd.* Panel (a): Experimental desorption rates, $\Phi/10^{-2}\mathrm{MLs}^{-1}$, deconvoluted into the Boltzmann component Φ_B and $\Phi_{asd} = \Phi - \Phi_B$, plotted as a function of σ. The examined system is Pd(foil) at T = 380K and T = 466K. Panel (b): The *asd* component of the desorption rate, $\Phi_{\mathrm{asd}}/10^{-2}\mathrm{MLs}^{-1}$, is plotted as a function of σ for the Pd(foil) at T = 380K and at five different pressures (in 10^{-6}Pa units) marked in the figure (dotted lines). The dashed line is the pressure independent Boltzmann component, Φ_{B}, the full thick straight lines refer to Φ at $p/10^{-6}$ Pa = 1.3 and 13. The initial portion of the Φ curves (displayed as thin lines) marks the hypothetical transitions $\Phi_B \rightarrow \Phi_{asd}$.

experimental $K(\sigma)$ are well described by the exponential function $K(\sigma) = K(0)\exp(-b(T)\sigma)$ with $K(0)$ of the order 5×10^{14} s^{-1} and values of b increasing with temperature (table 2).The initial deviation from linearity of all curves follows from eqn.15 where $K(\sigma)\rightarrow\infty$ for $\Phi_{asd}\rightarrow 0$ when $\sigma\rightarrow 0$. Actually eqn.15 is valid for steady state non-equilibrium conditions that are only established after

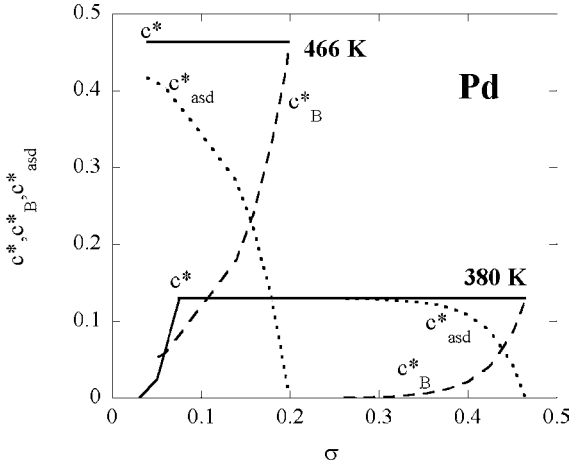

Fig. 8. CO *asd.* Relative population $c^*/10^{-15}$ of the vibrational level v^*, deconvoluted into the Boltzmann component c_B^* and $c_{asd}^* = c^* - c_B^*$, plotted vs. σ. Data refer to Pd(foil) at T = 380K and T = 466K ($p/10^{-6}$Pa = 2). The initial section of the c* curve at 380 K marks the transition $\Phi_B \rightarrow \Phi_{asd}$.

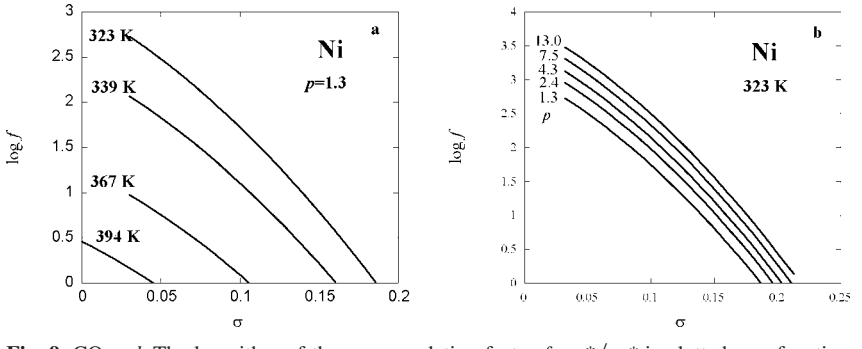

Fig. 9. CO *asd.* The logarithm of the *over*population factor $f = c^*/c_B^*$ is plotted as a function of σ for the Ni (foil) at $p/10^{-6}$Pa = 1.3 and at four different temperatures (panel a). In panel (b) the same quantity is displayed at T = 323K and at five different pressures.

a transition from initial Boltzmann conditions, where $\Phi = \Phi_B$, to non–equilibrium conditions, where $\Phi = \Phi_{asd} \gg \Phi_B$. This transition should occur at some value $\sigma_{tr} > 0$. The theoretical model predicts a sharp transition, as discussed in [24,25], and figs.7 and 8 show hypothetical transitions in the initial stages of the adsorp-

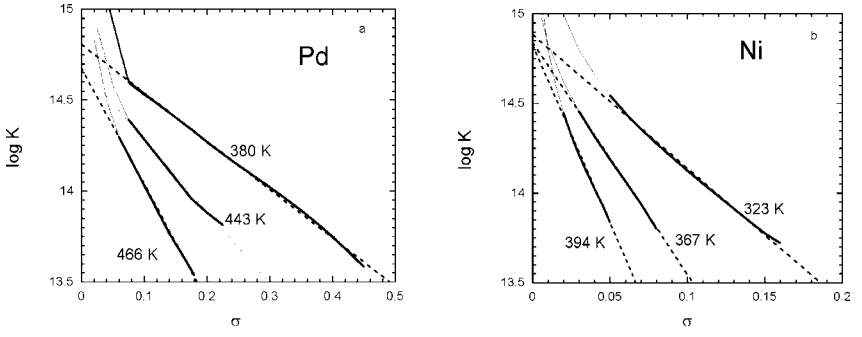

Fig. 10. CO *asd.* Panels (a-b). Log K plotted versus the fractional surface coverage σ for Pd and Ni at the temperatures indicated in the figures. Dashed lines are fits to the linear part of these plots.

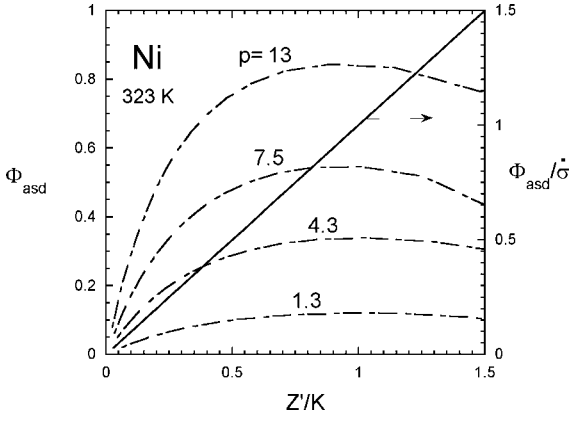

Fig. 11. CO *asd.* Ni (foil) at T = 323K and at the different pressures marked in the figure (in units 10^{-6}Pa). The behavior of the rate coefficient $\Phi_{asd}/10^{-2}$ s^{-1} as a function of Z'/K is displayed on the left scale. The straight line $\frac{\Phi_{asd}}{\dot{\sigma}} = \frac{Z'}{K}$ is shown on the right scale.

tion-desorption process. In fig.11 one plots Φ (left scale) and Φ/J (right scale) vs. $Z'/K(\sigma)$ at pressures from 1.3 to $13/10^{-6}$Pa, as derived for Ni at 323K.

It is well known that direct sticking of CO on metal surfaces according to a 'hit and stick' model doesn't account for the observed adsorption kinetics that can be described, on the other hand, by a 'precursor-mediated' adsorption model. Equations of the form of eqn.10 and 11 have in fact been derived from these models [26–32]. The chemisorption process under *asd* condition is, however, basically different from adsorption under Boltzmann conditions because of the close-coupling between $\dot{\sigma}$ and Φ which stems from the present analysis. In fact

Φ_{asd} is proportional to $\dot{\sigma}(\sigma)$ and is higher than Φ_B nearly up to equilibrium. Eqn.15 can be rewritten as

$$\dot{\sigma} = K\sigma^*_{asd} \tag{15}$$

which identifies $\dot{\sigma}$ with the probability per unit time, K, of the transition CO(v^*) $\rightarrow$ CO($v = 0$) multiplied by the *asd* surface coverage σ^*_{asd} of the CO(v^*) adspecies. This vibrationally excited adspecies could than be identified with the 'intrinsic precursor' of the aforementioned models. The shape of $\dot{\sigma}$ (σ), i.e. the value of m and n in eqns.10 and eqn.11, should then be related to $K(\sigma)$, and the decrease of m (or the increase of n) with the temperature should be linked to the increasing negative slopes at increasing temperature (Table 2).

Another consequence of the coupling between $\dot{\sigma}$ and Φ_{asd} is that J can't be given *a priori* by a model equation, as for J_B (e.g. $J_B = J_0(1-\sigma)$ for a 'hit and stick' model), but results from the sum $\Phi+\dot{\sigma}$ and this explains the presence of maxima in the $J(\sigma)$ curves of fig.5. This holds true also for the J curves of fig.1 and represents a distinctive feature of the non-equilibrium systems where desorption is enhanced by the *over*-population of the vibrational levels of the adsorbate, due to the interplay of energy disposal and reaction rates. In these systems the constraint is $\Phi + \dot{\sigma} = J(\sigma) \leq J(0)$. It is worth to remind that desorption rates measured under equilibrium conditions of the adsorption process have been found to coincide with those measured in vacuo, with no evidence for stimulation by adsorption at equilibrium [17]. This can now be understood because values of $\Phi_{asd}>0$ can only be expected when $c^* > c_B^*$, i.e. according to eqn.8, when $\dot{\sigma} > 0$, while at equilibrium, $\dot{\sigma} \equiv 0$. This should also follow from thermodynamic considerations: at true equilibrium there is no part of the system in which the distribution function is not Boltzmannian, while the onset of *asd* processes is bound to non-equilibrium distributions .

3. Discussion

The evidence for vibrational excitation in the H-Me adlayer stems from the time evolution of the three selected vibrational levels presented in ref.[8], by the validity of eqn.7 at s.s. (fig.4) and the $T/T_1 < 1$ values of Table1. In *asd* of CO, the evaluation of $\Phi_B(\sigma)$ allows one to deconvolute the linear dependence of the experimental Φ on σ into the $\Phi_{asd}(\sigma)$ and the $\Phi_B(\sigma)$ components (fig.7) and to show the dependence of $\Phi_{asd}(\sigma)$ on both temperature and pressure. The dependence on pressure is a distinctive feature of *asd*; in fact no pressure dependence can be expected for a desorption process in Boltzmann equilibrium. A convincing illustration of vibrational non-equilibrium in a CO-Me adlayer in the presence of adsorbing CO_{gas} is provided by both fig.8 for Pd and by fig.9 for Ni, where the relative population c^* of the performing level v^* is compared with the population c_B^* expected in the case of Boltzmann equilibrium.

In the formulation of section 1 of ref.[1] K is a phenomenological quantity, for it was defined without specifically addressing the physical process of energy

dissipation. The application of eqn.4 to a *rsd* process and of eqn.8 to *asd* provides a picture that is common to both systems: The rate coefficient for vibrational energy transfer to the surface K is a function of the surface coverage of the relevant adsorbate (H_s, CO_s) and can be expressed as a linear log K vs.σ function, with K values decreasing from the initial $K(0)$, of the order 10^{14}–$10^{15}s^{-1}$, down to K_{ss} at steady state of the order $10^{12}s^{-1}$ for *rsd* and of $10^{13}s^{-1}$ for *asd.* These orders of magnitude of the *Ks* should correspond, as mantained in [1], to non-adiabatic processes of energy exchange between adsorbate and metal electron gas, recently discussed in the literature [33,34]. The control parameters of the desorption rates Φ are in all cases $Z/K(\sigma)$ and $J(\sigma)$ or $\dot{\sigma}$ (σ). This dependence is illustrated by the Φ/J vs. Z/K plots of fig.3 and by the $\Phi_{asd}/\dot{\sigma}$ vs. Z'/K straight line of fig.11. This figure highlights the role of $\dot{\sigma}$ (σ) by showing how Φ vs. Z'/K plots, corresponding to different pressures, all merge into the straight line of the $\Phi_{asd}/\dot{\sigma}$ plots.

The decrease of K with increasing surface coverage represents the open problem linked to the application of the model to treat experimental data. In paper [1] an expression for K was derived for energy dissipation *via* electron-hole pair excitation and it is given by eqn.3 above. K is therefore made up of two terms, the first is related to the electron density available at the surface, $n_e^{2/3}$, and the second to the transition probability for electron excitation above the Fermi level $\Gamma_{\Delta E}\Delta E$. The decrease of K could then be attributed to the well-established decrease of n_e caused by the adsorbate. The surface electron density has to be considered, in general, a function of the total surface coverage, σ, for the surface electron density does in fact change during the adsorption process. The expression of K at surface coverage 0 and σ reads,

$$K(0) \propto n_e^{2/3}(0)\Gamma_{\Delta E(0)}\Delta E(0) \quad \text{and}$$

$$K(\sigma) \propto n_e^{2/3}(\sigma)\Gamma_{\Delta E(\sigma)}\Delta E(\sigma).$$

Consequently

$$K' = \frac{K(\sigma)}{K(0)} = \left(\frac{n_e(\sigma)}{n_e(0)}\right)^{2/3} \frac{\Gamma_{\Delta E(\sigma)}\Delta E(\sigma)}{\Gamma_{\Delta E(0)}\Delta E(0)} = X\Gamma' \tag{16}$$

The density of surface electrons in equilibrium with the metal scales according to $n_{e,s} \propto e^{-\beta W_s}$ where W_s is the energy contribution to the work function of the surface dipole layer. The change of the metal work function is then equal to $\Delta\phi = W_s(\sigma) - W_s(0) \approx W_{exp}\ \sigma$. A value $\Delta\phi = 0.17\sigma/\text{eV}$ is available for the Ni(100)-H system [9] and literature values of $\Delta\phi$ eV, at surface saturation by CO, are: Pd-CO, 0.9±0.1[20]; Ni-CO, 1.3±0.2 [21]; Rh-CO, 1.0±0.1 [22,23]. We shall then write $X = (\frac{n_e(\sigma)}{n_e(0)})^{2/3} = \exp(-\frac{2}{3}\beta W_{\exp}\sigma)$ and $\Gamma'(\sigma) = \frac{\Gamma_{\Delta E(\sigma)}E(\sigma)}{\Gamma_{\Delta E(0)}E(0)}$.

Eqn.16 reads $\log\Gamma' = \log K'(\sigma) - \log X$ and one derives $\Gamma'(\sigma)$ from the experimental log $K(\sigma)$ plots. For *asd*-CO the knowledge of $E_a(\sigma)$ (fig.6) allows one to study the behavior of log Γ' as a function of $E_a(\sigma)$. This is shown in fig.12 for Pd, Ni and Rh at different temperatures. From these linear plots one

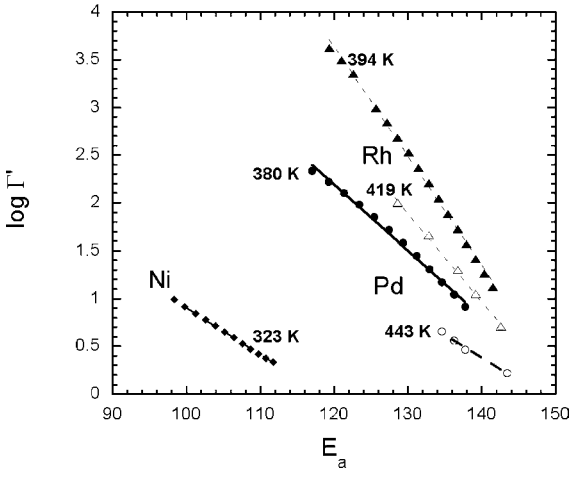

Fig. 12. CO *asd.* logΓ' plotted vs. $E_a(\sigma)$ for Pd , Ni and Rh at various temperatures.

receives $\Gamma' \propto 10^{-gE_a(\sigma)}$ where the g values have been collected in table 2. With $E_a(\sigma) \approx 6E_{01}(\sigma)$ one gets $\Gamma' \propto 10^{-gE_{01}(\sigma)}$. In conclusion the observed dependence of K on σ can be written as

$$\log \frac{K(\sigma)}{K(0)} = -(0.29\beta W_{\exp}\sigma + 6gE_{01}(\sigma)). \tag{17}$$

For the Ni(100)-H system at 120 K use of eqn.17 provides, for reasonable $E_a(\sigma)$ functions, values of g of the order 0.1–0.15 mol kJ^{-1}. This phenomenological equation shows the two components of $K(\sigma)$, one bound to the decrease of the electron density at the surface, caused by the increased surface density of the adsorbate, the other related to an increased transition probability bound to a vibrational quantum $E_{01}(\sigma)$ that decreases with σ. At T = 466 K for Pd and T = 367 K for Ni, log K' = log X, within the uncertainties of the experimental data, so that log Γ' ≈ 0, i.e Γ' becomes nearly independent of σ. This observation and the g values of table 2 suggest that g should be a decreasing function of temperature.

The complexity of the process of energy transfer from adsorbing species to the metal electron gas under reaction conditions and the limits of the available experimental data prevent, at present, reaching the level of understanding of the problem that would be required for a fully convincing interpretation of the observed dependence of K on σ.

The possible role played by metal phonons in the process of energy dissipation has not been considered so far, because the basic assumption of the analysis implies a prevailing dissipation via e-h pair excitation. In the case of Me-H adlayers this assumption is correct because experimental K values of the order 10^{12}-10^{13} s^{-1}(fig.2) should be compared with literature values of the order of

10^8-$10^9 s^{-1}$ accepted for vibrational relaxation of Me-H bonds via phonon excitation. Values of K of the order of 10^{13}-10^{14} s^{-1} for Me-CO adlayers (fig.10) should be compared with literature figures of the order 10^{10}-$10^{11} s^{-1}$ estimated for Pt-CO, while values for Ni-CO could actually be larger due to a smaller E_a values (fig.6). However, also in the case of the Ni-CO system dissipation via phonon excitation should not prevail, because the observed dependence on temperature is opposite to that expected for dissipation via phonons [35] as well as the observed decrease with σ.

The analysis is now being extended to Me-O adlayers, such as those present in N_2O decomposition or in CO oxidation at low pressure in the high-rate regime. Preliminary results provide convincing evidence for vibrational excitation of these adlayers, as well as for an increase of K at decreasing surface coverage by oxygen, i.e. at increasing n_e.

4. Conclusions

The existence of non-Boltzmann reaction regimes controlled by parameters other than activation energy and temperature, predicted by the theoretical model [1], has been ascertained in two systems. Rates of desorption in vibrationally excited Me-H and Me-CO adlayers are controlled by the ratio $Z \,/\, K(\sigma)$, with $K(\sigma)$ a decreasing function of σ, and by $J(\sigma)$ or $\dot{\sigma}$ (σ), both dependent on gas pressure. These reaction regimes are defined by steady-state vibrational distribution functions of the adspecies characterised by an *over*population of the levels with respect to Boltzmann equilibrium. The adopted model should thus be classified as a 'hot atom' scheme in that it provides the extra concentration ($c^* - c_B^*$) of the active 'hot adspecies' $A(v^*)$, as determined by parameters proper of the process of energy dissipation into the metal.

The assumption of a prevailing e-h pair excitation mechanism for disposal of the energy set free in these processes might provide a rationale to the decrease of K with increasing σ observed in both systems but certainly requires additional evidence.

References

1. E. Molinari, M. Tomellini, Z. Phys. Chem. **224** (2010) 743.
2. E. Molinari, M. Tomellini, Surf. Sci. **601** (2007) 1.
3. S. Whener, J. Küppers, J. Chem. Phys. **108** (1998) 3353.
4. J. Y. Kim, J. Lee, J. Chem. Phys. **113** (2000) 2856.
5. Th. Biederer, Th. Kammler, J. Küppers, Chem. Phys. Lett. **286** (1998) 15.
6. Th. Kammler, J. Lee, J. Küppers, J. Chem. Phys. **106** (1997) 7362.
7. Th. Kammler, J. Küppers, J. Chem. Phys. **111** (1999) 8115.
8. E. Molinari, M. Tomellini, Surf. Sci. **600** (2006) 273.
9. K. Christmann, O. Schober, G. Ertl, F. M. Neumann, J. Chem. Phys. **60** (1974) 4528.
10. T. Yamada, T. Onishi, K. Tamaru, Surf. Sci. **133** (1983) 533; Surf. Sci. **157** (1985) L389.

11. T. Yamada, K. Tamaru, Surf. Sci. **138** (1984) L155.
12. T. Yamada, K. Tamaru, Z. Phys. Chem. **144** (1985) 195.
13. N.Takagi, J. Yoshinobu, K. Kawai, Phys. Rev. Lett. **73** (1994) 292.
14. T. Yamada, K. Tamaru, Surf. Sci. **146** (1984) 341.
15. P. W.Tamm, L. D. Schmidt, J. Chem. Phys. **52** (1970)1150.
16. J. Weber, K. J. Laidler, J. Chem. Phys. **19** (1951) 1089.
17. M. Sushchikh, J. Lauterbach, W. H. Weinberg, Surf. Sci. **393** (1997) 135.
18. G. Ertl, Adv. Catal. **45** (2000)1.
19. M.Hassel, J.Chem. Phys. **114** (2001) 530.
20. H. Conrad, G. Ertl, E. E. Latta, Surf. Sci. **43** (1974) 462.
21. K. Christmann, O. Schober, G, Ertl, J.Chem. Phys. **60** (1974) 4719.
22. C. T. Campbell, G. Ertl, H. Kuipers, J.Segner, Surf. Sci. **107** (1981) 207.
23. C. M. Mate, C. T. Kao, G. A. Somorjai, Surf. Sci. **206** (1988) 145.
24. M. Tomellini, Surf. Sci. **556** (2004) 184; *ibid* **557** (2005) 200; Physica A **369** (2006) 369.
25. E. Molinari, M.Tomellini, Surf. Sci.**552** (2004)180; Catalysis Today **116** (2006) 30,56.
26. G. Ehrlich, J. Phys. Chem. **59** (1955) 473.
27. P. J. Kisliuk, J. Phys. Chem.Solids. **3** (1957) 95; **5** (1958) 78.
28. R. P. H. Gasser, E. B. Smith, Chem. Phys. Lett.**1** (1967) 457.
29. A. Cassuto, D. A. King, Surf. Sci. **102** (1981) 388.
30. H. J. Kreuzer, J. Chem. Phys. **104** (1996) 9593.
31. S. McEwen, S. H. Payne, H. J. Kreuzer, M. Kinne, R. Denecke, H. P. Steinrück, Surf. Sci. **545** (2003) 47.
32. S. H. Payne, J. S. McEwen, H. J. Kreuzer, D. Menzel, Surf. Sci. **594** (2005) 240.
33. C. Frischkorn, M. Wolf, Chem. Rev. **106** (2006) 4207.
34. K. Watanabe, D. Menzel, N. Nilius, H. J. Freund, Chem. Rev. **106** (2006) 4301
35. B. N. J. Persson, Ph. Avouris, Surf. Sci. **390** (1997) 45; B. N. J. Persson, J. W Gadzuk, Surf. Sci.**410** (1998) L779.